Journal of Alloys and Compounds 509 (2011) 10032–10035

Contents lists available at ScienceDirect

Journal of Alloys and Compounds

journal homepage: www.elsevier.com/locate/jallcom

Microwave absorption properties of TiN nanoparticles

Rui Liu, Ning Lun, Yong-Xin Qi, Yu-Jun Bai*, Hui-Ling Zhu, Fu-Dong Han, Xiang-Lin Meng, Jian-Qiang Bi, Run-Hua Fan

Key Laboratory for Liquid–Solid Structural Evolution and Processing of Materials (Ministry of Education), Shandong University, Jinan 250061, PR China

ARTICLE INFO

Article history:
Received 13 December 2010
Received in revised form 5 June 2011
Accepted 5 August 2011
Available online 12 August 2011

Keywords:
Nanoparticles
Titanium nitride
Microwave absorbing
Amorphous layer

ABSTRACT

TiN nanoparticles with an average diameter of 15 nm or so were prepared by the reaction of spongy Ti and NH_4Cl at about 530 °C. The electromagnetic parameters of the TiN nanoparticles/wax composite were measured by a coaxial line method. The nanoparticles exhibit good microwave absorbing ability owing to dielectric loss, and the measured reflection loss reaches a minimum value of −16.1 dB at 13.8 GHz. The interfaces between nanocrystalline TiN and the thin amorphous TiO_2 layer on the TiN surface contribute dominantly to the high permittivity and good microwave absorbing properties.

© 2011 Elsevier B.V. All rights reserved.

1. Introduction

Electromagnetic (EM) wave absorbing materials have extensive and significant applications for EM interference shielding and radar cross section reduction. Recently, an increasing interest has been focused on nano-sized materials owing to the better EM absorbing properties than bulk absorbers [1]. For instance, Fe nanowires with diameters of 70–200 nm could markedly reduce the eddy current loss and exhibited an outstanding EM wave absorption in the frequency range of 5.6–18 GHz [1]. Magnetic nanoparticles encapsulated in carbon nanotubes (CNTs) exhibited better EM absorption properties between 2 and 18 GHz [2–4], and the CNTs filled with ferromagnetic nanowires might be used as lightweight microwave absorbers [5,6]. Mn_3O_4 nanoparticles exhibited excellent microwave absorbing properties with a minimum reflection loss (RL) of −27.1 dB at 3.1 GHz [7]. Porous Fe_3O_4/SnO_2 and $Fe_3O_4/Fe/SiO_2$ core/shell nanorods possessed good EM absorbing properties due to the effective complementarities between the dielectric loss and the magnetic loss [8,9]. Silicon carbide nanoparticles doped with nitrogen exhibited excellent EM wave absorption properties with a minimum RL of −43.15 dB at 12 GHz and with a single layer of 3 mm in thickness [10].

Very recently, Meng et al. [11] studied the EM wave absorption properties of carbon coated TiC nanocubes, and the RL exceeded −20 dB in the frequency range of 6–16 GHz. Owing to the similarity in structure between TiC and TiN, it is reasonable to speculate that TiN may also exhibit good EM wave absorption properties.

TiN is an important material with a lot of excellent properties, such as extreme hardness, high chemical and thermal stability, good thermal and electrical conductivity [12], and can be utilized in harsh environments. In this work, TiN nanoparticles were synthesized using spongy Ti and NH_4Cl as reactants, whose EM properties were determined by measuring the relative complex permittivity ($\varepsilon_r = \varepsilon' - j\varepsilon''$) and permeability ($\mu_r = \mu' - j\mu''$) of the TiN/paraffin wax composite.

2. Materials and methods

TiN nanoparticles were synthesized using spongy Ti and NH_4Cl as reactants, a method similar to that in the literature [13]. In a typical procedure, 2.4 g spongy Ti and 3.0 g NH_4Cl were put into a stainless autoclave of 30 mL capacity. Then the autoclave was sealed and heated in a furnace to 530 °C and maintained for 10 h. When the autoclave was cooled to ambient temperature naturally, solid product with golden color was obtained (Fig. S1 in supplementary data), which almost maintained the shape of the original spongy Ti. However, the product was very fragile and could be triturated in an agate mortar. The product was washed successively with anhydrous ethanol, dilute hydrochloric acid and deionized water several times to remove the residual reagents and the byproduct, and then dried at 60 °C for 10 h. The yield of the resulting product was about 87 wt.% based on the starting material of spongy Ti.

The X-ray diffraction (XRD) pattern of the resulting product after washing was obtained on a Rigaku Dmax-rc diffractometer with Ni-filtered Cu Kα radiation (V = 50 kV, I = 80 mA) at a scanning rate of 4°/min. The morphology of the TiN was examined by using a JSM-6700F field emission scanning electron microscope (FESEM), and the microstructure by a Tecnai 20U-Twin high-resolution transmission electron microscope (HRTEM). Infrared (IR) spectra were measured by a BRUKER VECTOR 22 FT-IR spectrometer.

The EM absorbing properties of the TiN nanoparticles were determined by measuring the relative complex permittivity and permeability of TiN/wax composite. A toroidal shaped sample (φ_{out} = 7 mm, φ_{in} = 3 mm) was prepared by mixing 50 wt.%

* Corresponding authors. Tel.: +86 53188392677; fax: +86 53188392315.
E-mail address: byj97@126.com (Y.-J. Bai).

0925-8388/$ – see front matter © 2011 Elsevier B.V. All rights reserved.
doi:10.1016/j.jallcom.2011.08.022

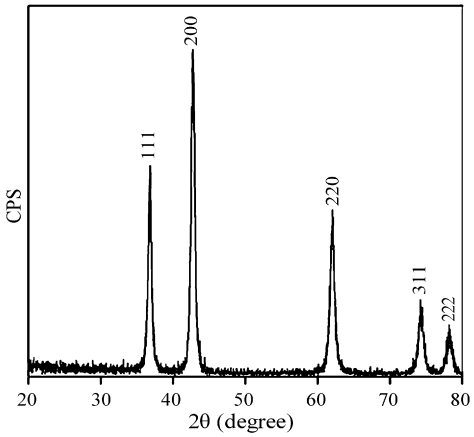

Fig. 1. XRD pattern of the resulting product after washing.

TiN nanoparticles with wax uniformly. The relative complex permittivity and permeability of the sample were measured using a coaxial line method in the frequency range of 2–18 GHz by an E8363B PNA Series Network Analyzer. To achieve the actual values of RL versus frequency, we further fabricated another TiN/wax composite containing 30 wt.% of nanocrystalline TiN, which was coated on an aluminum plate of 180 mm × 180 mm in size. The thickness of the composite is 5 mm. The RL versus frequency was measured by a HP 8757E scalar Network Analyzer in the frequency range of 2–18 GHz.

3. Results and discussion

Spongy Ti is the primary product with porous structure in Ti industry. Using the spongy Ti as reactant to prepare TiN is not only cost-saving but also highly efficient because the high porosity is favorable to the transport and diffusion of reactants, thus promoting the reaction rate. Furthermore, Ti is an important element in nitriding alloys, and the appropriate nitriding temperature range under NH_3 atmosphere is 500–570 °C at which a number of active nitrogen atoms generate. As a consequence, the formation of TiN nanoparticles in this work involves two concomitant and synergetic reactions: the directly nitriding of Ti and the reaction between Ti and HCl to form titanium chlorides which further reacted with NH_3 to produce TiN [13]. The former is conducive to maintaining the shape of the original spongy Ti, and the latter contributes to forming TiN nanoparticles. The golden color of the solid product (Fig. S1) is an indication of the formation of TiN. Meanwhile, the etching effect of HCl on the walls of spongy Ti resulted in highly fragile TiN which could be easily triturated into powders in an agate mortar.

From the XRD pattern shown in Fig. 1, all the diffraction peaks can be indexed to face-centered cubic (fcc) TiN (fm $\bar{3}$ m space group) with a calculated lattice constant a = 4.244 Å, which is in good agreement with that in JCPDF Card No. 38-1420 (a = 4.241 Å). No other impurities are detectable in the XRD pattern. The broadening of the peaks is indicative of the formation of nanocrystalline TiN with an average size of about 15 nm calculated by Scherrer's equation.

From the FESEM image displayed in Fig. 2a, the TiN nanoparticles are uniform in diameter, which can be further confirmed by HRTEM (Fig. 2b). The average diameter of the TiN nanocrystals is about 15 nm, consistent with the value calculated from the XRD pattern. The inset at bottom left of Fig. 2b is the corresponding electron diffraction pattern (EDP) of the TiN nanocrystals, the diffraction rings correspond to the (1 1 1), (2 0 0), (2 2 0), (3 1 1), and (2 2 2) planes of fcc TiN. Fig. 2c is the lattice fringe image of the TiN nanocrystals, the lattice spacing of 0.21 nm is close to that between two adjacent (2 0 0) planes of the fcc TiN, and a thin amorphous layer with loose structure can be observed around the TiN nanoparticles. Taking into account of the high surface energy of nano-sized TiN and the thermodynamics ($2TiN + 2O_2 = 2TiO_2 + N_2$, $\Delta rG_m^{\Theta} = -1160.5$ kJ mol^{-1}), the nanocrystalline TiN might be slightly oxidized under ambient atmosphere, so the amorphous layer is TiO_2, which could be further verified by IR spectra (Fig. 2d). The absorption band in the range of 880–450 cm^{-1} corresponds well to the characteristic vibrational modes of TiO_2 [14].

The relative complex permittivity and permeability of the TiN nanoparticles/wax composite were measured using a coaxial line method. The real (μ') and imaginary parts (μ'') of permeability are shown in Fig. 3a. Their values are about 1.0 and 0.0, respectively, suggesting that TiN is a nonmagnetic material and little magnetic loss will occur. Fig. 3b displays the real (ε') and imaginary (ε'') parts of the permittivity and dielectric loss tangent of the composite. It can be seen that the curves for the real and imaginary parts are almost flat only with some fluctuations occurring at 10.7 and 15.3 GHz. The fluctuations are perhaps related to displacement current lag at the interface between TiN nanocrystals and the thin amorphous TiO_2 layers [15]. The main part of ε' is around 8.9, and that of ε'' around 0.5. The high permittivity of TiN nanocrystals might arise from the interfacial polarization of the heterogeneous structure between TiN nanocrystals and the thin amorphous TiO_2 layers [16–18]. For further clarifying whether the enhanced permittivity is aroused by interfacial polarization or by TiO_2, we performed an oxidation experiment to fully oxidize TiN nanocrystals into pure TiO_2 (Fig. S2 in supplementary data) by heating the nanocrystals in air at 600 °C for 2 h, and measured the permittivity of TiO_2. As shown in Fig. 4a and b, pure TiO_2 does not exhibit higher permittivity than the nanocrystalline TiN, that is, the high permittivity of TiN nanocrystals is not resulted from the permittivity of TiO_2 layer. Furthermore, the TiN nanocrystals slightly oxidized at 250 °C for 10 min exhibits obviously enhanced complex permittivity (Fig. 4a and b) as compared to both the nanocrystalline TiN and the pure TiO_2. Similarly, the interfacial polarization caused by the thin amorphous TiO_2 layer and the nanocrystalline TiN is conducive to the enhancement of the complex permittivity. As is known, TiN is a good conductor with large quantity of conducting electrons. When incident EM wave travels through the surface of nanocrystalline TiN, the conducting electrons under electric field will result in electric current, producing Ohm loss which is another contribution to the permittivity [18,19]. Meanwhile, the nanocrystalline TiN possesses a large specific surface area of 73 m^2 g^{-1} (Fig. S3 in supplementary data), so numerous defects present on the surface of TiN, which could act as polarization centers under the EM field, also giving rise to an increase in the permittivity [20,21].

Fig. 5a shows the simulation of RL versus frequency with different coating thicknesses according to the transmission line theory [22]. The absorption peaks shift to lower frequencies with increasing the coating thickness. A second peak appears when the thickness is more than 5 mm, and a third one occurs when the thickness reaches 8 mm. Two weak peaks around 10.7 and 15.3 GHz in Fig. 5a are consistent with those in Fig. 3b, suggestive of the interdependence between these peaks. Meanwhile these peaks do not change their positions with varying coating thickness, and thus should result from the interfacial polarization owing to the large surface area of the TiN nanocrystals. The TiN nanoparticles/wax composite reaches a minimum RL of −15.3 dB at 15.9 GHz and an absorption bandwidth lower than −10 dB of 0.8 GHz with a coating thickness of 8 mm. Fig. 5b displays the actual RL value versus frequency by measuring the plate of nanocrystalline TiN/wax composite. The minimum RL value is −16.1 dB at 13.8 GHz and the absorption bandwidth lower than −10 dB is 1.7 GHz. The positions of the absorbing peak are well consistent with the calculated ones (Fig. 5a), however, the absorption intensity is higher and the absorption

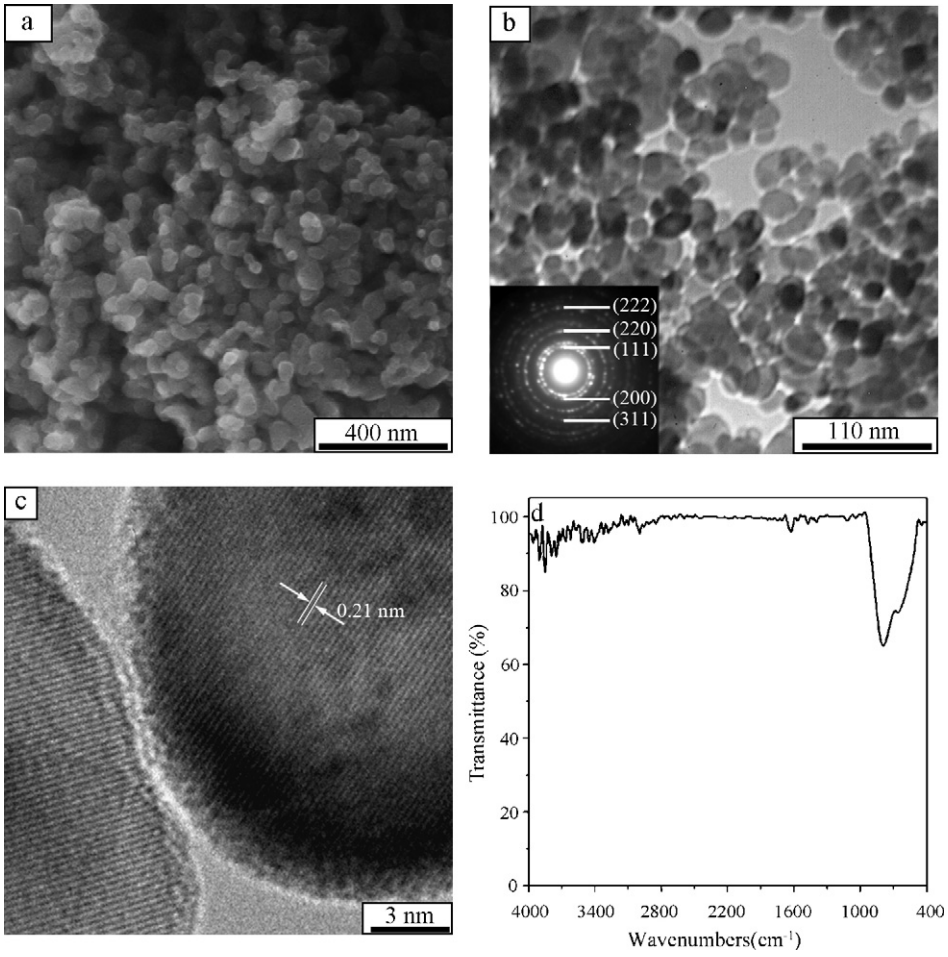

Fig. 2. FESEM (a), HRTEM (b), lattice fringe (c) images and IR spectra (d) of the resulting TiN nanocrystals. The inset in (b) is the corresponding EDP.

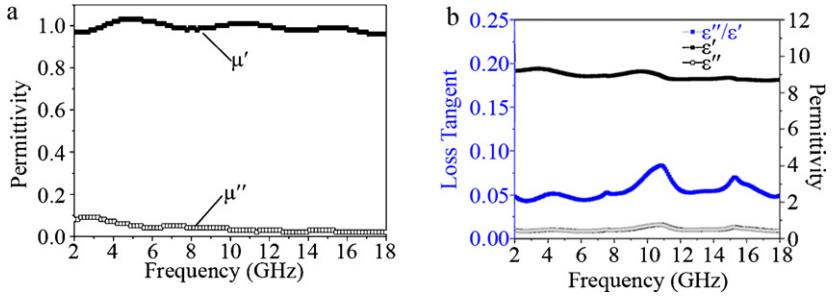

Fig. 3. Relative complex permeability (a) and permittivity and dielectric loss tangent (b) of the TiN nanoparticles/wax composite versus frequency.

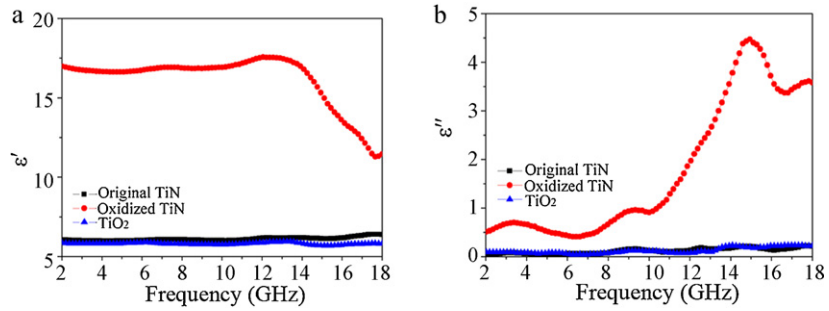

Fig. 4. Real part (a) and imaginary part (b) of the relative complex permittivity of the original TiN, oxidized TiN and pure TiO_2 compositing with wax versus frequency, respectively.

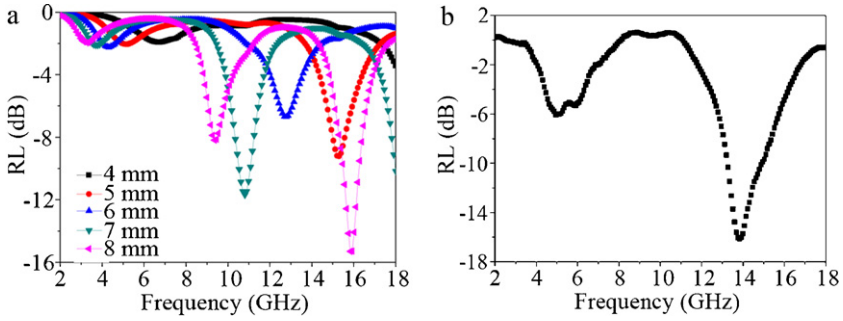

Fig. 5. Simulation of RL for the composites with different thicknesses (a), measured value of the TiN/wax composite with 5 mm thickness (b).

bandwidth is wider than the simulation result, indicating that the TiN nanoparticles indeed exhibit good EM absorbing properties.

4. Conclusions

In conclusion, TiN nanoparticles exhibits good microwave absorbing properties due to dielectric loss, which includes interfacial polarization, Ohm loss and defect polarization loss. The measured RL could reach a minimum value of −16.1 dB at 13.8 GHz and the absorption bandwidth lower than −10 dB is 1.7 GHz. Coupled with the excellent properties of TiN, the composites containing TiN nanoparticles could be used as good microwave absorbers and may find wide applications under harsh circumstances requiring high abrasion and wear resistance.

Acknowledgements

This work was supported by the National Natural Science Foundation of China (Nos. 50972076 and 50872072), Shandong Provincial Natural Science Foundation, China (Y2008F26 and Y2008F40), Science and Technology Development Project of Shandong Province (2009GG10003001 and 2009GG10003003), and Special Fund for Postdoctoral Innovative Project of Shandong Province (200702024).

Appendix A. Supplementary data

Supplementary data associated with this article can be found, in the online version, at doi:10.1016/j.jallcom.2011.08.022.

References

[1] J.R. Liu, M. Itoh, M. Terada, T. Horikawa, K.I. Machida, Appl. Phys. Lett. 91 (2007) 093101.
[2] R.C. Che, L.M. Peng, X.F. Duan, Q. Chen, X.L. Liang, Adv. Mater. 16 (2004) 401–405.
[3] D.L. Zhao, X. Li, Z.M. Shen, J. Alloys Compd. 471 (2009) 457–460.
[4] D.L. Zhao, J.M. Zhang, X. Li, Z.M. Shen, J. Alloys Compd. 505 (2010) 712–716.
[5] R.T. Lv, F.Y. Kang, J.L. Gu, X.C. Gui, J.Q. Wei, K.L. Wang, D.H. Wu, Appl. Phys. Lett. 93 (2008) 223105.
[6] T.C. Zou, H.P. Li, N.G. Zhao, C.S. Shi, J. Alloys Compd. 496 (2010) L22–L24.
[7] D. Yan, S. Cheng, R.F. Zhuo, J.T. Chen, J.J. Feng, H.T. Feng, H.J. Li, Z.G. Wu, J. Wang, P.X. Yan, Nanotechnology 20 (2009) 105706.
[8] Y.J. Chen, P. Gao, R.X. Wang, C.L. Zhu, L.J. Wang, M.S. Cao, H.B. Jin, J. Phys. Chem. C 113 (2009) 10061–10064.
[9] Y.J. Chen, P. Gao, C.L. Zhu, R.X. Wang, L.J. Wang, M.S. Cao, X.Y. Fang, J. Appl. Phys. 106 (2009) 054303.
[10] D.L. Zhao, F. Luo, W.C. Zhou, J. Alloys Compd. 490 (2010) 190–194.
[11] H. Meng, K. Song, H. Wang, J. Jiang, D. Li, Z. Han, Z. Zhang, J. Alloys Compd. 509 (2011) 490–493.
[12] P. Patsalas, S. Logothetidis, J. Appl. Phys. 90 (2001) 4725–4734.
[13] X. Yang, C. Li, B.J. Yang, W. Wang, Y.T. Qian, Mater. Res. Bull. 39 (2004) 957–962.
[14] Y.J. Hu, C.Z. Li, F. Gu, Y. Zhao, J. Alloys Compd. 432 (2007) L5–L9.
[15] X.G. Liu, D.Y. Geng, H. Meng, P.J. Shang, Z.D. Zhang, Appl. Phys. Lett. 92 (2008) 173117.
[16] N. Bowler, IEEE Trans. Dielectr. Electr. Insul. 13 (2006) 703–711.
[17] C.C. Lee, D.H. Chen, Appl. Phys. Lett. 90 (2007) 193102.
[18] S.W. Phang, M. Tadokoro, J. Watanabe, N. Kuramoto, Curr. Appl. Phys. 8 (2008) 391–394.
[19] L.J. Deng, M.G. Han, Appl. Phys. Lett. 91 (2007) 023119.
[20] P.C.P. Watts, W.K. Hsu, A. Barnes, B. Chambers, Adv. Mater. 15 (2003) 600–603.
[21] D. Zhao, X. Li, Z. Shen, Mater. Sci. Eng. B 150 (2008) 105–110.
[22] E. Michielssen, J.M. Sajer, S. Ranjithan, R. Mittra, IEEE Trans. Microwave Theory Tech. 41 (1993) 1024–1031.